10.1002/chem.201900492

COMMUNICATION

Conformational Dynamics Underlies Different Functions of Human KDM7 Histone Demethylases

Shobhit S. Chaturvedi, [&][a] Rajeev Ramanan, [&][a] Sodiq O. Waheed,[a] Jon Ainsley,[b] Martin P. Evison,[b] Jennifer M. Ames,[c] Christopher J. Schofield,[d] Tatyana G. Karabencheva-Christova,[*][a,b] and Christo Z. Christov.[*][a,b]

Abstract: The human KDM7 subfamily histone H3 Nε-methyl lysine demethylases PHF8 (KDM7B) and KIAA1718 (KDM7A) have different substrate selectivities and are linked to genetic diseases and cancer. We describe experimentally based computational studies revealing that flexibility of the region linking the PHD finger and JmjC domains in PHF8 and KIAA1718 regulates inter-domain interactions, the nature of correlated motions, and ultimately H3 binding and demethylation site selectivity. F279S an X-linked mental retardation mutation in PHF8 is involved in correlated motions with the iron ligands and second sphere residues. The calculations reveal key roles of a flexible protein environment in productive formation of enzyme-substrate complexes and suggest targeting the flexible KDM7 linker region is of interest from a medicinal chemistry perspective.

The methylation states of Lys- and Arg-residues on histones can have profound effects on the structures and functions of chromatin, with consequences for expression in healthy and diseased tissues. [1a,2] Methyl transferases and demethylases regulate histone methylation status. The largest family of Nε-methyl Lys-demethylases (KDMs) belongs to a superfamily of non-heme Fe (II) dependent oxygenases, which catalyze a wide range of reactions including hydroxylations, deoxygenations, ring formations, halogenations, and demethylations, normally coupled to 2-oxoglutarate (2OG) cosubstrate oxidation. [1a,2,3]

PHF8 (KDM7B) and KIAA1718 (KDM7A) are human Jumonji C (JmjC) family 2OG-dependent Nε-methyl lysine demethylases. Overexpression of KDM genes is linked to various cancers, including prostate,[4,5] breast,[6] laryngeal and hypopharyngeal,[7] non-small cell lung,[8] and oesophageal cancer.[9] Substitution of Phe279 for serine in PHF8 is associated with inherited X-linked mental retardation.[1a,10-12] PHF8 and KIAA1718 specifically act on the Nε-dimethylated lysine residues of the histone H3 N-terminal tail. Crystal structures of PHF8/KIAA1718 reveal an unusually simple two domain architecture for JmjC KDMs, indicating they are good models for understanding molecular details of KDM function; both have single JmjC domain and single plant homeodomain (PHD) finger (Figure 1). Their JmjC domain has a double stranded beta-helix core fold (DSBH), which, as in other 2OG oxygenases, harbors a non-heme Fe (II) active site which binds the dimethylated lysine of the preferred H3 histone H3K9me2 (PHF8) or H3K27me2 (KIAA1718) substrates (Figure S1). The PHD fingers of both bind to H3K4me3, promoting catalysis at H3K9me2 in the case of PHF8 and at H3K27me2 for KIAA1718 (Figure 1).[1a,1b] The two domains communicate via a linker region (aa 66 -78 in PHF8; 98-113 in KIAA1718), the flexibility of which is proposed to be important in determining differences in selectivity between PHF8 and KIAA1718.[1b] The KIAA1718 linker contains three more residues than that of PHF8 and is proposed to orient the substrate in an extended conformation across both domains that enables selective demethylation at $H3_{1-35}$ K4me3-K27me2).[1b]

Despite crystallographic insights, the molecular details underlying the strikingly different site selectivity of PHF8/KIAA1718, have been unclear. We describe molecular dynamics (MD) simulations of 1μs each on PHF8 and KIAA1718, in complex with Fe (II), 2OG, and their H3 histone substrates. Combined Quantum Mechanical and Molecular Mechanical (QM/MM) characterization of enzyme-substrate complexes was used to reveal the effects of the protein environment on the reactant complex in PHF8. The overall results reveal the importance of conformational dynamics of the region linking the PHD finger and JmjC domains in determining selectivity.

MD simulations of PHF8 complexed with Fe(II), 2OG, and its $H3_{1-14}$K4Me3-K9Me2 substrate, reveals the latter is flexible and capable of adopting a more extended conformation than observed crystallographically (Figure 2A, S18). The orientation of the H3K9me2 side chain in the PHF8 active site is stabilized by interactions with S192 and I191, consistent with the crystal structure. Interactions that bind and orientate the H3K9me2 two methyl groups are stable – one H3K9me2 methyl group (Met1, Figure 1B) is positioned to make hydrophobic interactions with the Y234/L236 side chains; the second methyl group (Met2) is proximate with oxygens of the iron ligating D249 and the N333 side chain.[1b] The distances between Met1 and Met2 and Fe(II) are stable with Met2 being closer (Figure 2B). The distribution of the torsion angles for Met1 and Met2 with the lysine H3K9 side chain carbons manifest average values of -108° and 67°, suggesting restricted rotation about the CE-NZ bond of H3K9me2 (Figure S2). A stable hydrogen bond (in ~70% of MD snapshots) between NZ of H3K9me2 and O1 of 2OG is involved in restricting free rotation of Met1 and Met2 in the PHF8 active site. MD studies with KDM4A (JMJD2A), which acts on H3K9me3/2, also indicate restricted rotation of substrate N-methyl groups.[13] The distribution of Met2 group within 4.7Å of Fe (II) is ~77% and for Met1 group is ~6%, implying Met2 is more favorably positioned than Met1 for demethylation.

[a] Department of Chemistry, Michigan Technological University, Houghton, Michigan 49931, USA. E-mail: christov@mtu.edu, tatyanak.mtu.edu
[b] Faculty of Health and Life Sciences, Northumbria University, Newcastle upon Tyne, NE1 BST, UK.
[c] Centre for Research in Biosciences, University of West of England, Coldharbour Lane, Bristol, BS16 1QY, UK.
[d] The Chemistry Research Laboratory, Mansfield Road, University of Oxford, OX1 5JJ, UK.
[&] S.S.C. and R.R. made equal contribution to this article.

Supporting information for this article is given via a link at the end of the document.

10.1002/chem.201900492

COMMUNICATION

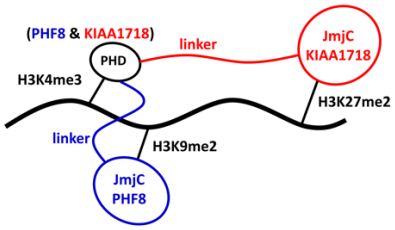

Figure 1. Schematic representation of interactions of domains in PHF8 (blue) and KIAA1718 (red) with histone H3.

In the PHF8 MD simulations, the H3K4me3 side chain is positioned to make extensive cation-π interactions with the PHD finger side chains of Y7, Y14, and W29, which form a hydrophobic cage. The H3K4me3 side chain also interacts with M20, I21 and S354, as observed crystallographically (Figure 2C). Details of the interactions of histone peptide with PHF8 are given in the SI (Table S1, S2).

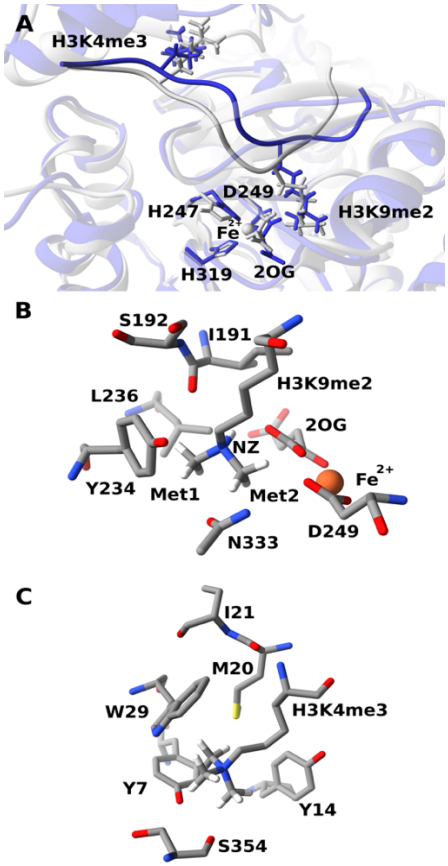

Figure 2. Binding of H3K4me3-K9me3 ($H3_{1-14}$) to PHF8. (A) Comparison of the conformation as observed in the MD cluster (blue) with that observed crystallographically (PDB: 3KV4) (silver) for PHF8. (B) H3K9me2 (M2L) interactions in PHF8. (C) H3K9me3 (M3L) interactions with the PHD finger of PHF8. Selected hydrogen atoms only are shown for clarity.

The KDM7 2OG and Fe(II) binding sites are (Figure S3) located within the DSBH core fold, with the metal non-coordinating 2OG C5 carboxylate penetrating deep into the DSBH.[2] In PHF8, the electrostatic interaction of the 2OG C5 carboxylate with side chain of K264 (a characteristic feature of JmjC KDMs)[1b,4,14] remains stable during the MD (Figure S4). Hydrogen bonds between the 2OG C-5 carboxylate oxygens and Y257 (in 74% of the MD snapshots) and T244 (52%) are stable during the MD; however, the hydrogen bonds with N189 (5%) show more limited stability (Figure 3). In KIAA1718, the 2OG C5 carboxylate makes analogous interactions with K299, Y292 (93%), T279 (27%), and N224 (5%) (Figure. 3). The simulations with both enzymes suggest that while the 2OG binding site is conformational stable overall, some flexibility exists; this may be important in controlling dioxygen activation during catalysis.

The PHD domains of PHF8 and KIAA1718 manifest similar flexibilities as indicated by their average RMSD values of 2.7 Å and 2.5 Å, respectively (Figure. S5). Both JmjC domains are more stable (RMSDs 1.8Å and 1.5Å) than the PHD fingers (Figure. S5). Such stability might be important in maintaining the orientation of the co-substrates during catalysis. The DSBH fold is the most stable element within the JmjC domain (Figure S5) (RMSDs 1.3Å and 0.6Å for PHF8 and KIAA1718 respectively) in agreement with its role in enabling a stable non-heme Fe (II) environment.

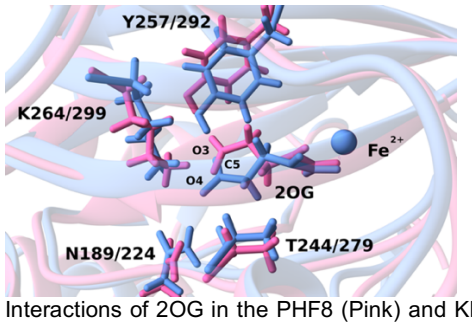

Figure 3. Interactions of 2OG in the PHF8 (Pink) and KIAA1718 (Blue) active sites. Residues labelled as 1-letter code PHF8/KIAA1718.

The linker region in PHF8 is not observed in reported crystal structures[1b] in agreement with this, the MD simulations imply the PHF8 linker is relatively flexible whilst that of KIAA1718 is much more rigid (Figure. S6). This difference may relate to the role of the linker in PHF8 in enabling conformational plasticity for effective demethylation at H3K9me2, in contrast to KIAA1718 where binding at H3K4me2 hinders activity at H3K9me2.[1b] Notably, the radius of gyration of the linker region of PHF8 shows a decreasing trend, suggesting that the linker moves towards a more bent conformation, so adjusting the positions of the PHD and JmjC domains for substrate binding at H3K9me2 as shown in previous experimental reports.[1b] With KIA1718, the linker stays in an extended conformation as observed in the crystal structure (Figure. S7) keeping the both domains in an orientation that does not allows for proper binding of H3K9me2. [1b]

To investigate the network of collective correlated motions in the two KDM7s we applied Dynamic Cross Correlation Analysis (DCCA) (Figure. S8). For PHF8, the DCCA indicates positive correlations within the PHD domain which may contribute to domain stability; negative (anti-) correlations were observed with the JmjC domain; these could help produce flexible linker mediated interactions between the two domains that assist in substrate binding. The linker region itself showed anti-correlations with both PHD and JmjC domains, reflecting the flexible connection between the domains and their more autonomous adjustments around the respective substrate binding sites. The

COMMUNICATION

DSBH motif showed positive correlated motions among its residues which correlate with its conformational stability. The substrate H3K9me2 residue showed a strong positive correlation with S192 and the backbone of the histone peptide (A458-S462). H3K4me3 shows strong positive correlation with PHD domain residues (Y15-I21, H31 and E39) and part of the histone peptide (A452-T457). The collective motions involving the H3 peptide might facilitate productive substrate binding to both PHD and JmjC domains. The PHF8 F279S substitution abolishes catalytic turnover and is linked to X-linked mental retardation. [1a,10-12] F279S shows a strong positive correlation with the Fe-coordinated histidines, aspartate and neighboring residues (PHF8 244-248, 317-320) and a strong positive correlation with second sphere residues (267-300), but a negative correlation with the linker region. These results imply the importance of collective motions for the integrity of the JmjC domain and the active site. The collective motions in KIAA1718 are more intense than in PHF8 (Figure. S9), possibly due to the difference in the nature of the two linker regions - the more rigid linker in KIAA1718 may enable better coupling of motions between the two domains. Further, the linker might control not only the mutual orientation of the two domains, but also the mechanics of their internal collective motions. Principal Component Analysis (PCA) of PHF8 shows a substantial contribution from the linker region and minor one from the PHD finger to the main direction of motion; whilst in KIAA1718 the main contribution comes from the PHD finger and the linker region is rigid, in agreement with the experimental studies[1b] (Figure. 4, S11).

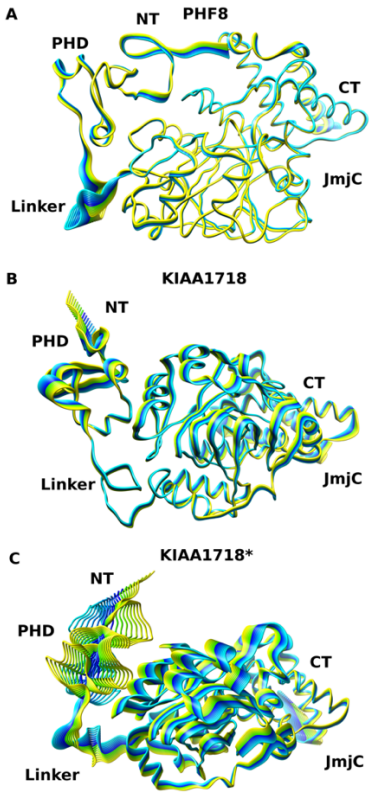

Figure 4. Principle component analysis showing the direction of motion in (A) PHF8 and (B) KIAA1718 (C) KIAA1718*. Yellow to blue represents the direction of motion of protein residues. N- and C-Terminal regions are labelled as NT and CT, respectively.

To further explore the effect of the linker on interactions between the two domains we created an in silico chimeric KIAA1718 (KIAAA1718*) containing the PHF8 linker, by removing the natural linker from KIAA1718 and inserting the PHF8 linker. KIAA1718* shows higher RMSD of C-alpha atoms than wild type KIAA1718, likely reflecting changes in conformation to accommodate the new linker. KIAA1718* also becomes more flexible overall, due to introduction of the PHF8 linker (Figure. S12). The radius of gyration (Rg) of the linker in KIAA1718* shows that it equilibrates to a more bent conformation as compared to KIAA1718 (Figure. S13). Thus, the center of mass distance between PHD and JmjC domains of KIAA1718* shows a tendency to decrease, compared to KIAA1718 (Figure. S14). PCA analysis of KIAA1718* shows a significantly increased contribution to the first principal component form the inserted linker region (Figure. 4), consistent with increased flexibility compared to wild type. These results provide in silico support for the relatively flexible nature of the PHF8 linker which allows the PHD finger to bind at H3K4me3 and the JmjC domain to bind H3K9me2. In the case of KIAA1718 there is a more rigid linker and more open conformation which, despite PHD:H3K4me3 binding, does not productively accommodate H3K9me2. [1b]

To explore the effect of conformational flexibility on the structures of the reactant complex at atomistic and electronic structural levels, we performed QM/MM geometry optimizations on five structural snapshots, i.e. 300ns, 600ns, 700ns, 800ns and 1000ns of the PHF8 MD trajectory. Geometry optimization calculations were performed using Density Functional Theory (DFT) and unrestricted BP86 with 10 % exact HF (Hartree Fork) exchange functional. The 6-311G* basis set was used for Fe and its first coordinating atoms (oxygen and nitrogen) from the imidazole and carboxylate ligands. 6-31G* was employed for the rest of the atoms in QM region. The use of unrestricted BP86 with a 10% exact HF functional has been experimentally validated for application to non-heme iron enzymes.[15] QM/MM optimization of an MD snapshot of PHF8 shows that the triplet state of Fe (S=1, M=3) is higher in energy by ~14 kcal than the quintet state (S=2, M=5), which is in agreement with other QM/MM studies on the related KDM4A JmjC enzyme and experimental reports on non-heme enzymes.[16,17] Hence, all further QM/MM calculation in this study were done on the quintet spin state of Fe.

The geometric features of the Fe center with its coordinated ligands and co-substrates presented in the MD simulations are maintained in the enzyme-substrate complex structures of PHF8 after QM/MM optimization (Figure 5 and Table S3). The non-heme iron is in the +2 oxidation state based on its spin density of ~3.8 which corresponds to a +2 oxidation state. These results agree with the CD/MCD spectroscopy experiments performed on the active sites of other 2OG dependent enzymes. [18-20] The average distance of Met2 to the Fe (II) is 5.1Å in the QM/MM minimized snapshots and the distance of Met1 to Fe (II) is 5.6 Å. The dihedral angle (CD: CE: NZ: Met2 and CD: CE: NZ: Met1) of the H3K9me2 peptide in QM/MM minimizations manifests averaged values of 65° and -119° (Table S4), in comparison to 67° and -108° in the MD simulations. The 2OG C5 carboxylate is stabilized by binding to K264 in both MD and QM/MM optimized snapshots (Table S5). The QM/MM studies support the presence of stabilizing CHO type hydrogen bond interactions between the methyl group Met2 of the H3K9me2 with the side chains of D249 and N333 (Table S6).

The comparison between the QM only optimized cluster of PHF8 containing the Fe (II) with coordinated ligands and co-

COMMUNICATION

substrates with the QM/MM optimizations of PHF8, including the protein environment shows a difference in the orientation of the two methyl groups. The QM cluster does not account for steric effects and interactions experienced from the protein environment. Thus, in the QM cluster both N-methyl groups are near equidistant from the Fe center, while the QM/MM calculations show that one methyl group is closer to Fe center than the other (Figure. S15, Table S3). Thus, in agreement with other studies of non-heme iron enzymes, [21] the protein environment enables productive orientation of reactive groups in the enzyme-substrate complex of PHF8.

The five QM/MM optimized MD snapshots of PHF8 show similar overall geometries but manifest small differences, indicating the QM/MM calculation outcomes depend on the starting geometry (Figure 5). This is consistent with the concept that in large flexible catalysts, the reactant complexes are not single structures, but ensembles; thus, it is probably important to use multiple starting structures in reaction path calculations. [22,23]

The QM/MM optimizations, using both mechanical and electronic embedding within the subtractive scheme (with the ONIOM method), provide consistent results, both between themselves and with respect to the QM/MM optimizations using the additive scheme and electrostatic embedding (ChemShell) (Figure. S16, Table S3). The results suggest that long-range electrostatics might not play considerable effects on the geometric features of the reactant complex, in agreement with QM/MM calculations of other non-heme iron enzymes. [22] This proposal, however, does not imply that long-range electrostatic effects are not important in determining reaction paths, transition states and energy barriers.

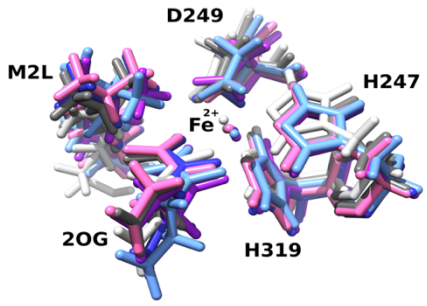

Figure 5. Superimposed QM/MM optimised geometries showing flexibility and movement at the active site of PHF8. H3K9me2 is labelled as M2L.

Crystallographic and biochemical/kinetic studies on KDM7 enzymes[1b] raise questions about how their protein environment and its dynamics control their different selectivities. MD studies, supplemented by QM/MM calculations, reveal that differences in the flexibilities of the linkers in PHF8 and KIA1718 control the different inter-domain orientations of the PHD and JmjC domains, thus enabling catalytically productive binding of H3K9me2 at the JmjC domain when H3K4me3 is presented by the PHF8 PHD. A network of correlated motions facilitates substrate binding and contributes to the internal stabilities of the PHD and JmjC domains. The flexibility of the linker in addition to the effect on the inter-domain orientation influences correlated motions in PHF8 and KIAA1718, leading to a more intensively correlated system in KIAA1718. Phe-279, substitution of which in the case of F279S in PHF8 correlates with X-linked mental retardation, [1a,10-12] participates in a correlated network involving the iron ligands and second sphere residues of the JmjC domain. By contrast with the flexibility involved in substrate binding, the geometry of the Fe center is stable, as are most interactions in the 2OG-binding site, likely in order to assure effective catalysis. [24]

Overall the results reveal the importance of linker dynamics in determining KDM7 substrate selectivity and reaction outcomes. They highlight the importance of considering the overall protein environment in calculations concerning the reaction geometries of KDM7 and, by implication, related enzymes involved in epigenetic regulation. The insight into KDM7 catalysis provided using MD and QM/MM methods is also of relevance to the design of modulators of PHF8 and KIAA1718 catalysis. In particular, they imply that modulating the system of correlated motions may be productive from the perspective of developing JmjC KDM isoform-selective inhibitors and, potentially, molecules that enhance of activity.

Keywords: KDM7 • Histone Demethylation • Molecular Dynamics • QM/MM

[1] a) C. Loenarz, W. Ge, M. L. Coleman, N. R. Rose, C. D. O. Cooper, R. J. Klose, P. J. Ratcliffe and C. J. Schofield, *Hum Mol Genet*, **2010**, *19*, 217–222. b) J. R. Horton, A. K. Upadhyay, H. H. Qi, X. Zhang, Y. Shi and X. Cheng, *Nat. Struct. Mol. Biol.*, **2010**, *17*, 38–44.
[2] C. J. Schofield and Z. Zhang, *Curr. Opin. Struct. Biol.*, **1999**, *9*, 722–731.
[3] X. Cheng and R. C. Trievel, in *2-Oxoglutarate-Dependent Oxygenases, RSC*, Edited by C. J. Schofield and R. P. Hausinger, **2015**, *vol. 2015–January*, pp. 210–245.
[4] M. Björkman, P. Östling, V. Härmä, J. Virtanen, J.-P. Mpindi, J. Rantala, T. Mirtti, T. Vesterinen, M. Lundin, A. Sankila, A. Rannikko, E. Kaivanto, P. Kohonen, O. Kallioniemi and M. Nees, *Oncogene*, **2012**, *31*, 3444–3456.
[5] Q. Ma, Z. Chen, J. Xueqiang, X. Xie and W. Jin, *Onco. Targets. Ther.*, **2015**, *8*, 1979–1988.
[6] Q. Wang, S. Ma, N. Song, X. Li, L. Liu, S. Yang, X. Ding, L. Shan, X. Zhou, D. Su, Y. Wang, Q. Zhang, X. Liu, N. Yu, K. Zhang, Y. Shang, Z. Yao and L. Shi, *J. Clin. Invest.*, **2016**, *126*, 2205–2220.
[7] G. Zhu, L. Liu, L. She, H. Tan, M. Wei, C. Chen, Z. Su, D. Huang, Y. Tian, Y. Qiu, Y. Liu and X. Zhang, *Epigenomics*, **2015**, *7*, 143–153.
[8] Y. Shen, X. Pan and H. Zhao, *Biochem. Biophys. Res. Commun.*, **2014**, *451*, 119–125.
[9] X. Sun, J. J. Qiu, S. Zhu, B. Cao, L. Sun, S. Li, P. Li, S. Zhang and S. Dong, *PLoS One*, **2013**, *8*, e77353.
[10] F. E. Abidi, M. G. Miano, J. C. Murray and C. E. Schwartz, *Clin. Genet.*, **2007**, *72*, 19–22.
[11] A. M. Koivisto, S. Ala-Mello, S. Lemmelä, H. A. Komu, J. Rautio and I. Järvelä, *Clin. Genet.*, **2007**, *72*, 145–149.
[12] F. Laumonnier, S. Holbert, N. Ronce, F. Faravelli, S. Lenzner, C. E. Schwartz, J. Lespinasse, H. Van Esch, D. Lacombe, C. Goizet, F. P. D. Tuy, H. Van Bokhoven, J. P. Fryns, J. Chelly, H. H. Ropers, C. Moraine, B. C. J. Hamel and S. Briault, *J. Med. Genet.*, **2005**, *42*, 780–786.
[13] O. Ulucan, O. Keskin, B. Erman and A. Gursoy, PLoS One, **2011**, *6*, e24664.
[14] J.-F. Couture, E. Collazo, P. A. Ortiz-Tello, J. S. Brunzelle and R. C. Trievel, *Nat. Struct. Mol. Biol.*, **2007**, *14*, 689–695.
[15] G. Schenk, M. Y. M. Pau and E. I. Solomon, *J. Am. Chem. Soc.*, **2004**, *126*, 505–515.
[16] W. A. Cortopassi, R. Simion, C. E. Honsby, T. C. C. França, and R. S. Paton, *Chem. Eur. J.,* **2015**, 21, 18983-18992.
[17] C. Krebs, D. G. Fujimori, C. T. Walsh, and J. M. Bollinger Jr., *Acc. Chem. Res.,* **2017**, 40, 484-492.

COMMUNICATION

[18] E. G. Pavel, J. Zhou, R. W. Busby, M. Gunsior, C. A. Townsend and E. I. Solomon, *J. Am. Chem. Soc.*, **1998**, *120*, 743–753.

[19] J. Zhou, W. L. Kelly, B. O. Bachmann, M. Gunsior, C. A. Townsend, E. I. Solomon, S. U. V, V. Recei, V. No, V. Re, M. Recei and V. May, *J. Am. Chem. Soc.*, **2001**, 7388–7398.

[20] M. L. Neidig and E. I. Solomon, *Chem. Commun.*, **2005**, *0*, 5843-5863.

[21] N. Proos Vedin and M. Lundberg, *J. Biol. Inorg. Chem.*, **2016**, *21*, 645–657.

[22] C. Z. Christov, A. Lodola, T. G. Karabencheva-Christova, S. Wan, P. V Coveney and A. J. Mulholland, *Biophys. J.*, **2013**, *104*, L5-7.

[23] D. Usharani, C. Zazza, W. Lai, M. Chourasia, L. Waskell and S. Shaik, *J. Am. Chem. Soc.*, **2012**, *134*, 4053–4056.

[24] C. Schofield and R. Hausinger, Eds., *2-Oxoglutarate-Dependent Oxygenases*, Royal Society of Chemistry, Cambridge, **2015**.

10.1002/chem.201900492

Entry for the Table of Contents (Please choose one layout)

Layout 1:

COMMUNICATION

The linker region in KDM7s regulates inter-domain interactions, the nature of correlated motions, and ultimately H3 binding and demethylation site selectivity.

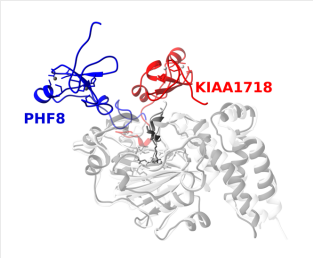

*Author(s), Corresponding Author(s)**

Page No. – Page No.

Title